Current Journal of Applied Science and Technology

Volume 42, Issue 42, Page 19-35, 2023; Article no.CJAST.108047
ISSN: 2457-1024
(Past name: British Journal of Applied Science & Technology, Past ISSN: 2231-0843, NLM ID: 101664541)

Prospects for the Characterization of the Fundamental Parameters Linked to the Energy Spectrum of the Aeolian Sea State in Benin Coastal Zone

Bernard N. Tokpohozin [a,b,c*], Djonoumawou M. G. F. Chidikofan [c], Fernando Y. J. Kpomahou [d], Christian D. Akowanou [a,c], Mathias A. Houékpohéha [b], Guy H. Hounguè [e] and Basile B. Kounouhéwa [b,e]

[a] Institut National Supérieur des Classes Préparatoires aux Etudes d'Ingénieur (INSPEI / UNSTIM) d'Abomey, République du Bénin.
[b] Institut de Mathématiques et de Sciences Physiques (IMSP/UAC) 01BP 613 Porto- Novo), République du Bénin.
[c] Laboratoire des Sciences, Ingénierie et Mathématiques (LSIMA/UNSTIM), Abomey, République du Bénin.
[d] Ecole Normale Supérieure de l'Enseignement Technique (ENSET/UNSTIM) de Lokossa BP 133 Lokossa, République du Bénin.
[e] Département de Physique (FAST) et Formation Doctorale Sciences des Matériaux (FDSM / UAC), République du Bénin.

Authors' contributions

This work was carried out in collaboration among all authors. All authors read and approved the final manuscript.

Article Information

DOI: 10.9734/CJAST/2023/v42i424270

Open Peer Review History:
This journal follows the Advanced Open Peer Review policy. Identity of the Reviewers, Editor(s) and additional Reviewers, peer review comments, different versions of the manuscript, comments of the editors, etc are available here: https://www.sdiarticle5.com/review-history/108047

Original Research Article

Received: 02/09/2023
Accepted: 09/11/2023
Published: 16/11/2023

**Corresponding author: E-mail: donaelfreed@gmail.com;*

ABSTRACT

The Beninese coast, like most coastal regions, is subject to various hydrodynamic factors that are likely to be modified by climate change. On the coast, the coasts are constantly subject to the action of waves, currents and wind. This work, carried out near the port of Cotonou, aims to provide representative statistics on the direction of the fundamental parameters of the wind seas, their height in the area close to the coast, where the swell is not yet subject to the action of the funds. Based on in situ data measurements with mooring systems at tide gauge - meteorological stations during the hydrodynamic measurement campaign and carried out at 10-minute time steps, on a regular basis over a period of four consecutive years by NORTECKMED in collaboration with the Millenium Challenge Account (MCA-Benin) within the framework of the extension of the Autonomous Port of Cotonou, the statistical distribution of the characteristic parameters of the waves (height, direction of propagation and period) is elaborated. Thus, the significant height $\mathrm{H_s}$, the peak period or the stable average wave period $\mathrm{T_p} \approx \mathrm{T_{m_s}}$ and the most frequent direction of propagation $\mathrm{D_p}$ are evaluated. A frequency characterization of the period $\mathrm{T_c}$, the wavelength $\mathrm{L_c}$ and the height $\mathrm{H_c}$ of short swells, generated by local winds, is obtained using the Pierson-Moskowitz frequency spectrum. In short, the four years of data made it possible to carry out statistical production and simulations of wind, tide and wave data in order to determine the significant heights $\mathrm{H_s}$, the peak period $\mathrm{T_p}$, the linear energy power available and the link between $\mathrm{H_s}$ and $\mathrm{T_p}$ according to the Beaufort scales. Likewise, we made a characterization of short swells (wind seas) based on the value of the local wind speed, the Pierson-Moskowitz frequency spectrum and a representation of the wave propagation directions.

Keywords: Significant wave height; wind sea conditions; wave direction; wave energy spectrum; coastal area of Benin.

ABBREVIATIONS

MCA : Millenium Challenge Account
IRHOB : Institute of Halieutic and Oceanological Research of Benin
CBRS I : Beninese Center for Scientific Research and Innovation

SCIENTIFIC NOTATION TABLES

v : Stable average wind speed on the fetch at $10m$ from the free ocean surface m/s.
ρ : Density of sea water (kg/m^3).
g : Gravity acceleration (m/s^2).
H_s : Significant crest-to-trough swell height (m).
H_{max} : Maximum crest-to-trough swell height (m).
H_{min} : Minimum crest-to-trough swell height (m).
H_c : Crest to trough height of short swell (m).
T_m: Mean swell period (s).
T_p: Peak swell period (s).
T_c : Short swell period (s).
L_c : Short swell wavelength (m).
C_g: Swell group speed (m/s).
C_φ : Swell phase speed (m/s).
$S_\omega(\omega, \vartheta)$: Pierson-Moskowitz wave energy spectrum.

1. INTRODUCTION

Waves are generated by the wind in the fetch zone. These waves smooth out to give more or less regular swells [1]. The waves or/and swells that we see propagating on the surface of oceans, seas or lakes are generally due to or generated by the effect of wind on the surface of the oceans [2]. The wind blowing across the sea surface transfers part of the energy from the atmosphere to the water surface. It is a phenomenon of friction of layers of air on the water which creates depressions on the crests and excess pressures in the troughs, having the effect of amplifying initial wavelets to form a complex regime of increasingly larger waves. Long and powerful as they spread. Strong winds of the West produce the largest waves in the world which initially move towards the West and are deflected towards the equator by the Coriolis effect, arriving from the North-West in the Northern Hemisphere and from the South-West in the South [3], [4]. The stronger it blows, for longer and over a greater distance, the greater the height of the waves generated. One of the predominant forcings of the ocean is swell. Characterizing the response of the water to a disturbance of its surface by the winds, it travels over many kilometers in deep seas, changes as

it approaches the coast before coming to rest on the beaches [5]. Since about forty years, Research on the study and understanding of the wave phenomenon has progressed considerably, both from a fundamental point of view and its application in coastal engineering, for example. The Mathematical theories, at the basis of all theoretical knowledge of the physical functioning of our environment, which deal with swell, have developed and become more complex [6], [7]. They represent a large quantity of phenomena linked to waves based on hypotheses developed from the general equations of fluid mechanics, and now make it possible to study ever more sophisticated problems analytically and numerically. Waves are common [8], and the longest wave swells generated in the global ocean can cross entire ocean basins before reaching the coastline [9]. The global swell climate was studied using the simulations model [10], but our knowledge of wave propagation are still limited by the scarcity of measurements [11], [12]. Empirical data support the idea that winds and swell together account for more than half of the energy carried by all waves at the ocean surface, exceeding the contribution of tides, tsunamis, coastal waves, etc [13]. These waves, gravity waves, have the particularity of propagating without dissipation of energy and can therefore travel long distances before being dissipated on the coasts. In addition, hydraulic physical models have become a great tool for supporting the calculations and simulations carried out with digital models, or replacing them when they find their limit, and representing processes related to the swell in a reduced model. Recent advances in terms of instrumentation and means of measuring phenomena have made it possible to represent the swell in a way that is ever closer to reality. Thus, channel wave generators now produce irregular swells, and tanks are more and more often equipped with “snake” type beaters, for example, making it possible to reproduce random multidirectional swells. Knowledge of wave and/or swell parameters and control of sea states are fundamental elements, both for the design and construction of coastal structures, for the estimation of the energetic power of waves and for forecasting. Maritime navigation and for the prevention and fight against coastal disasters [4], [14]. Waves are the most important phenomenon to consider among the environmental conditions affecting maritime structures, because they exert the greatest influence. Studies already carried out in the Gulf of Guinea have shown that three wave systems predominate in West Africa: the main and secondary swell, and the wind sea [15]. This observation is all the more true for the Beninese coast, exposed to particularly energetic swells in the coastal zone, than for the coastal countries of West Africa. [5]. The ocean is an environment rich in energy flows that can be exploited [16]. In terms of means of measurement, this portion of the Atlantic coast of the Gulf of Guinea has long been under-equipped. Indeed, non-directional measures are few in number and directional measures are rare and very recent. The incident direction of the swell is also a fundamental parameter in the calculation of coastal drift, capable of moving a significant quantity of sediment parallel to the coast [6]. Marine dynamics is a source of energy that is still poorly documented and therefore not exploited in Benin. Due to the random nature of waves, the sea state in general is described by statistical parameters, such as the average heights ($H_m \approx H_s$), the average of the periods ($T_m \approx T_P$) and the average of the propagation directions ($D_m \approx D_P$) [15]. Since the work of [17], the evolution of the sea state on time scales well beyond the wave period is based on the evolution of the energy or action spectrum (energy divided by the intrinsic frequency) [18]. One of these principles is used to predict the characteristics of short swells (wind seas) generated by local winds which often complicate the dynamics of waters on the coast. This work aims to fill the lack of information on the direction of the swells and to provide representative statistics of their heights in the deep-water zone, close to the coast, where the swell is not yet subjected to the action of the seabed. Statistical analysis shows that the port coast of Benin is strongly dominated by swell waves. The inter-annual variability of significant sea and swell wave heights, as well as how they relate to the resulting significant wave height, is analyzed over the study area. The main modes of variability of wind, sea and swell show notable differences.

2. MATERIALS AND METHODS

2.1 Presentation of the Study Area

Benin is a coastal state in the Gulf of Guinea which benefits from access to the ocean over a distance of approximately 125 km. Its coastal zone is between 6°13’ and 6°23’ north latitude (Fig. 1a). In this coastal zone, it receives an abundance of regular marine waves of low amplitude compared to their wavelength. [15]. Their amplitude varies depending on the time of

year on the one hand and on a daily basis on the other. In this area where gravity is $g = 9{,}79\ N/kg$ approximately, the density of the ocean is $\rho = 1025\ kg/m^3$ and we observe [16]: the dominant swells which are long swells having a period T ($8s \leq T \leq 18s$) whose stable mean value $T_m \approx 12s$ and a wavelength L_o approximately $220\ m$ in the deep waters of the coastal zone of the Gulf of Guinea [6], [15].

2.2 Data Sets Used

In-situ data : During a measurement campaign carried out over four consecutive years from June 2011 to April 2014 by NORTECKMED in collaboration with the Millennium Challenge Account (MCA) and the Autonomous Port of Cotonou, two measurement stations were anchored near the port of Cotonou, at a depth of $13.5m$ at the point of coordinates N6°20.118' and E2°27.257' (station WCP1) and $13m$ of depth at the point of coordinates N6°20.373' and E2°26.140' (station WCP2). This system is supplemented by a meteorological and tide gauge station installed in the port (Fig. 1b).

Anchorages: Each measuring station is equipped with an acoustic current and wave profiler (Accoustic Wave and Current Profiler; AWAC $1MHz$, Nortek). The wetted sensors recorded the directional parameters of the waves (significant height, direction and peak period) every 60 minutes at a frequency of $2Hz$ by the PUV method. The frequency spectrum of the swells, from which the significant height and the peak energy period are deduced, are determined. Peak directions are estimated from the horizontal components of the wave orbital velocities. Current data were recorded every 10 minutes, on 11 and 10 cells of $1m$ width each respectively at the first and second stations from $0.9m$ from the bottom towards the surface.

Tide gauge - meteorological stations: Sea level variations were recorded by a tide gauge (STS PTM/N/RS 485) positioned $75cm$ below the hydrographic datum located within the port enclosure at points N6°20.928' and E2°25.893'. The sensor used recorded the height of the water every 10 minutes at a frequency of $1Hz$. The wind data were recorded by an anemometer (WXT520 VAISALA) positioned $10m$ above the ground at points N6°20.554’ and E2°25.734’. The sensor used for this purpose recorded wind directions and speeds every 10 minutes.

2.3 Beaufort Scales in the Coastal Area

In order to characterize the different sea states in the coastal zone of Benin in the Gulf of Guinea, this work uses the Beaufort scales which characterize the swells in the deep waters near the coasts. These scales are summarized in the Table 1 [19], [20].

Fig. 1. Coastal zone and location of the port of Cotonou (Benin) with the various measurement stations. The two moorings (WCP1 and WCP2), the tide gauge station (TG) and meteorological station (WS and AN)

Table 1. Beaufort scales

Degree or strength	Appellation	Wave heights near the coast (m)	Sea states: (phenomenon observed at sea)	Wind speed (m/s)
B_0	Calm	0	Oil sea, mirror	≤ 1
B_1	Very light breezes	[0 – 0.1[	Sea wrinkled	[1.1 ; 2.5[
B_2	Beautiful	[0.1 – 0.15[	Ripples	[2. 5 ; 4[
B_3	Little agitated	[0.15 – 0.3[	Little sheep	[4 ; 6[
B_4	agitated	[0.3 – 0.46[	many sheep	[6 ; 8[
B_5	Strong	[0.46 – 0.76[	Waves, sea spray	[8 ;10.5 [
B_6	Very strong	[0.76 – 1.22[	Blades, crests of extended foam	[10.5 ; 15.5[
B_7	Fat	[1.22 – 1.68[	Breaking blades	[15. 5 ; 16[
B_8	Very fat	[1.68 – 2.29[	Crests of waves leaving in swirls of foam	[16 ; 18.5[
B_9	Huge	[2.29 – 3.05[	Spray obscuring the view, you can't see farther.	[18. 5 ; 21.5[
B_{10}	Storm	3.05 and more	- Very large blades with a long plume crest, the water surface appears white. Reduced visibility.	
			- The sea is entirely covered with banks of foam. Reduced visibility.	[21.5 ; 25[
			- The air is full of foam and spray. Significantly reduced visibility.	
			sea completely covered with banks of white foam, waves	
B_{11}	–	–	exceptionally high, very low visibility	[25 ; 29[
B_{12}	–	–	air full of foam and spray; banks of drifting foam, visibility almost zero	$\geq 29\ m \cdot s^{-1}$

2.4 Average Wind Speeds at Altitude z in the Study Area

Wind is a very complex aerodynamic phenomenon by nature. The wind speed v, in the Gulf of Guinea at Cotonou, varies between $3\,m/s$ and $8\,m/s$ approximately ($3\,m.s^{-1} \leq \vartheta_m \leq 8\,m.s^{-1}$) . Its stable average value ϑ_m is approximately $5\,m/s$ [4], [21].

If ϑ_m is the wind speed at an altitude z and ϑ_0 that corresponding to an altitude $h = 10m$, the vertical distribution of the speed is [22]:

$$\boldsymbol{\vartheta_m = \vartheta_0 \left(\frac{ln(z/z_0)}{ln(h/z_0)}\right) \approx \vartheta_0 \left(\frac{8{,}52+lnz}{10{,}5}\right)} \quad (1)$$

with $z_0 = 0{,}0002\ m$ on the water surface.

2.5 Characterization of Short Swells Generated by Local Winds

As has already been said, it is necessary to distinguish the sea from the wind due to the local action of the wind and the swell. The wind sea results from the combination of waves that propagate throughout the wind's area of action with locally created waves. Swell results from the propagation of waves from a generation zone, through areas where wind action is limited [23]. The Pierson-Moskowitz frequency spectrum is deduced from a series of measurements made in the Atlantic for established seas [19]. It corresponds to the region of gravity waves. It is also a function of the wind speed ϑ thanks to energy transfers according to Jeffrey's theory [22]. This spectrum is currently represented by one of the best empirical formulas available [8].

$$\boldsymbol{S_\omega(\omega,\theta) = \frac{2bg^2}{\pi\omega^5}\cos^2(\theta)\, e^{-\left(\frac{ag}{\omega\vartheta}\right)^4}} \text{ with } \begin{cases} a = -0{,}74 \\ b = 0{,}0081 \\ \omega = \frac{2\pi}{T} \end{cases} \quad (2)$$

Thus, in the coastal zone of the Gulf of Guinea, we have:

$$\boldsymbol{S_\omega(\omega,\vartheta) = S_f(T,\vartheta) = \frac{0{,}0243\ T^5}{\pi^5}\ e^{-0{,}74\left(\frac{g\,T}{2\pi\,\vartheta}\right)^4}}$$
$$\text{with } 3\,m.s^{-1} \leq \vartheta_m \leq 8\,m.s^{-1} \quad (3)$$

With this frequency spectrum, the period T_c of these short swells (wind seas) generated by local winds is given by:

$$\boldsymbol{T_c = \sqrt{\frac{m_o}{m_2}}} \quad \text{with} \quad \boldsymbol{m_n = \int_0^{+\infty} f^n S(f)\,df} = \boldsymbol{\int_0^{+\infty} \omega^n S(\omega)\,d\omega} \quad (4)$$

The zero-order moment $\boldsymbol{m_0 = \frac{bg^2}{-4a\omega^4} = \frac{0.0081*g^2}{4*0.74*\omega^4}}$ of the spectrum, represents the total surface energy density of the swell per unit of density of water. This period T_c corresponds to the maximum value of this frequency spectrum for a given wind speed.

$$\boldsymbol{T_c \quad \rightarrow \quad S_{f_{max}}(\vartheta, T_c) = \frac{0{,}0243\ {T_c}^5}{\pi^5}\ e^{-0{,}74\left(\frac{gT_c}{2\pi\,\vartheta}\right)^4}} \quad (5)$$

These waves thus generated by local winds, and which are not yet constrained to the action of the seabed, have a wavelength L_c [24]:

$$\boldsymbol{L_c = \frac{gT_c^2}{2\pi}} \quad (6)$$

The height of these short swells is given by: $H = 4\sqrt{m_o} = 4\sqrt{\int S(f)df}$: [24] ; [20], thus, we have :

$$\boldsymbol{H_c = 4\sqrt{\int \frac{0{,}0243}{\pi^5 f^5}\ e^{-0{,}74\left(\frac{g}{2\pi f\,\vartheta}\right)^4} df}} \quad \text{with} \quad 3\,m.s^{-1} \leq \vartheta \leq 8\,m.s^{-1} \quad (7)$$

In the shoaling zone, another expression of the Pierson-Moskowitz spectrum is widely used in the literature:

$$\boldsymbol{S_f(H_s, T_p) = \frac{5\,H_s^2}{16\,T_p^5 f^5}\ e^{\frac{-5}{4}\left(\frac{1}{T_p f}\right)^4}} \quad (8)$$

This frequency spectrum is characterized by two quantities:

- The peak period of the spectrum $\mathrm{T_p}$, for which the spectrum is maximum.
- The significant height $\mathrm{H_s}$, corresponds to an exact statistical definition, but it is simpler to remember that it also corresponds quite well with the height felt by seafarers [25]. By definition, this significant height $\mathrm{H_s}$ according to formula (2), is:

$$\boldsymbol{Aire = \left(\frac{H_s}{4}\right)^2 = \frac{2bg^2}{\pi}\int_{-\pi}^{\pi}\cos^2(\theta)\,d\theta \int_0^{+\infty}\frac{1}{\omega^5}e^{-\left(\frac{a\cdot g}{\omega\cdot v}\right)^4}d\omega} \quad (9)$$

According to the integration of expression (9), we have:

$$\boldsymbol{\left(\frac{H_s}{4}\right)^2 = \frac{b\cdot v^4}{2g^2a^4}} \quad \text{with} \quad \begin{cases} a = -0{,}74 \\ b = 0{,}0081 \\ g = 9{,}79 \end{cases} \Rightarrow \boldsymbol{H_s \approx 0{,}02 \cdot v^2} \quad (10)$$

With $\boldsymbol{v}$ the wind speed on the fetch at $10m$ from the free surface.

We have shown that the sea state is characterized by a constant pseudo-camber [26], we have :

$$\boldsymbol{H_s/(T_m)^2 = 0,0787} \quad (11)$$

If we assume like Gota Gota [20], $\boldsymbol{T_p = 1,29\, T_m}$ then expression (11) becomes:

$$\boldsymbol{H_s/(T_p)^2 = 0,0473} \quad (12)$$

By considering the irregular swell as a superposition of regular swells whose elementary amplitudes are given by the spectrum, it is again possible to calculate the power transported by the waves.

2.6 Application to Sea States : Sea State Energy Spectrum

In the Gulf of Guinea, swells are generally swells of low amplitude compared to their wavelength: they are Airy swells whose dispersion relation is:[15], [27], [28].

$$\boldsymbol{\omega^2 = gk\,tanh(kd)} \quad \text{with}$$

$$\begin{cases} L = \frac{2\pi}{k} & : \quad \text{The wavelength} \\ T = \frac{2\pi}{\omega} & : \quad \text{the period} \\ d & : \quad local\ water\ depth \end{cases} \quad (13)$$

The group velocity of Airy waves in deep water $(tanh(kd) \approx 1)$, is given by $C_g = \frac{\partial \omega}{\partial k} = \frac{gT}{4\pi}$ and the average of the mechanical energy $< E >$ of a significant swell amplitude H_s is $< E > = \frac{1}{8}\rho g {H_s}^2$. Thus, the energy power P of waves per unit of propagation length is the product of its total energy by its group speed [15], [29].

$$\boldsymbol{P = < E >.C_g = \frac{1}{32\pi}\rho g^2 {H_s}^2 T_p\, W/m = {H_s}^2 T_p\, KW/m} \quad (14)$$

By considering the irregular swell as a superposition of regular swells whose elementary amplitudes are given by the spectrum, it is again possible to calculate the power transported by the waves. We can see that the “drop” in linear power compared to a regular swell is 60% [30].

$$\boldsymbol{P = < E >.C_g = 0.4 {H_s}^2 T_p\ (KW/m)} \quad (15)$$

The following Table 2 gives some examples of this power transported for typical values of Hs and T_p considering expressions (12) and (15).

It can be seen that the level of energy carried by the waves is highly variable depending on the state of the sea, and can reach considerable power levels in the event of strong storms.

3. RESULTS AND DISCUSSION

3.1 Results Presentations

From in situ data measurements with mooring systems at the tide gauge - meteorological stations during the hydrodynamic measurement campaign and carried out at 10 minute time intervals, regularly over a period of four consecutive years (June 2011 to April 2014) by NORTECKMED in collaboration with the Millenium Challenge Account (MCA-Benin) as part of the extension of the Autonomous Port of Cotonou, we have:

- Produced statistics on the values of peak to trough wave heights according to the Beaufort scales near the coasts in order to identify the dominant sea states prevailing at the study site.
- Evaluated the annual distributions of these heights during each year in order to determine the significant heights H_s of these waves and evaluated their permanently available energy power.
- Define a typical day for each month by averaging measurements that are taken at the same time on all days of the month. This typical day allows us to know the variations in the almost stable values of these heights during the course of a day.
- Represented the distribution diagrams of the wave propagation directions and established the frequency and direction spectra of these swells as a function of the stable average wind speed on the site.
- Characterized short swells (wind seas) based on the value of local wind speed, the Pierson-Moskowitz frequency spectrum and the Beaufort scale.

The wind data (average direction and speed) were presented in Fig. 2. The curves, in Figs 2a and 2b, respectively reflect the variations in the direction of propagation and the variability of the wind speed in the Gulf of Guinea at Cotonou in the months of June, July and August 2011.

Table 2. Examples of the power transported for typical values of Hs and T_p

Beaufort scales	1	2	4	5	6	7	8	9	10	11	12
$H_s(m)$	0.2	0.7	1.7	3	4.7	6.8	9.3	12.1	15.3	18.9	22.9
$T_p(s)$	2	4	6	8	10	12	14	16	18	20	22
$P(KW/m)$	0.032	0.78	6.94	29	88.36	222	484	937	1685	2858	4615

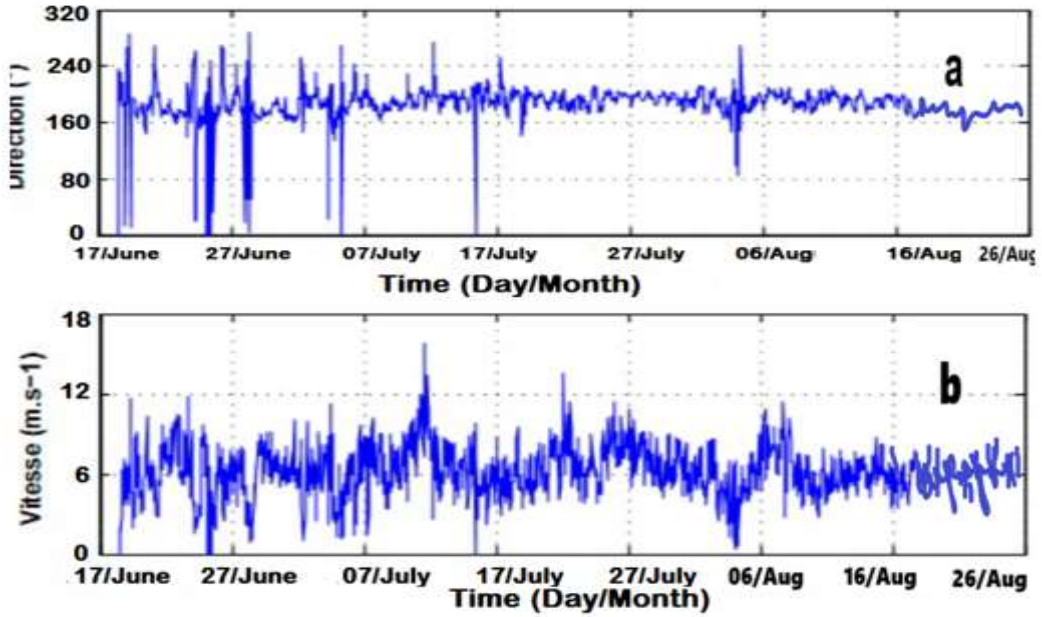

Fig. 2. Evolution of wind direction (a) and speed (b) recorded during the measurement campaign at the Cotonou port

The curves in Fig. 3 reveal the annual temporal statistical distribution of the hydrodynamic parameters measured during the measurement campaign at the port of Cotonou from 2011 to 2014. The data observed every hour of the parameters characterizing the state of the waves (significant height, direction peak and peak period) at the two anchorages from June to August 2011 are presented in Fig. 3. As well as those linked to the variation in sea level (tide) recorded every minute by the tide gauge.

The statistical representations in Fig. 4 below show the distribution of peak-to-trough wave height values in the Gulf of Guinea in Benin according to the Beaufort scales, near the coast, during each month. The empty months are those during which the measuring instruments failed.

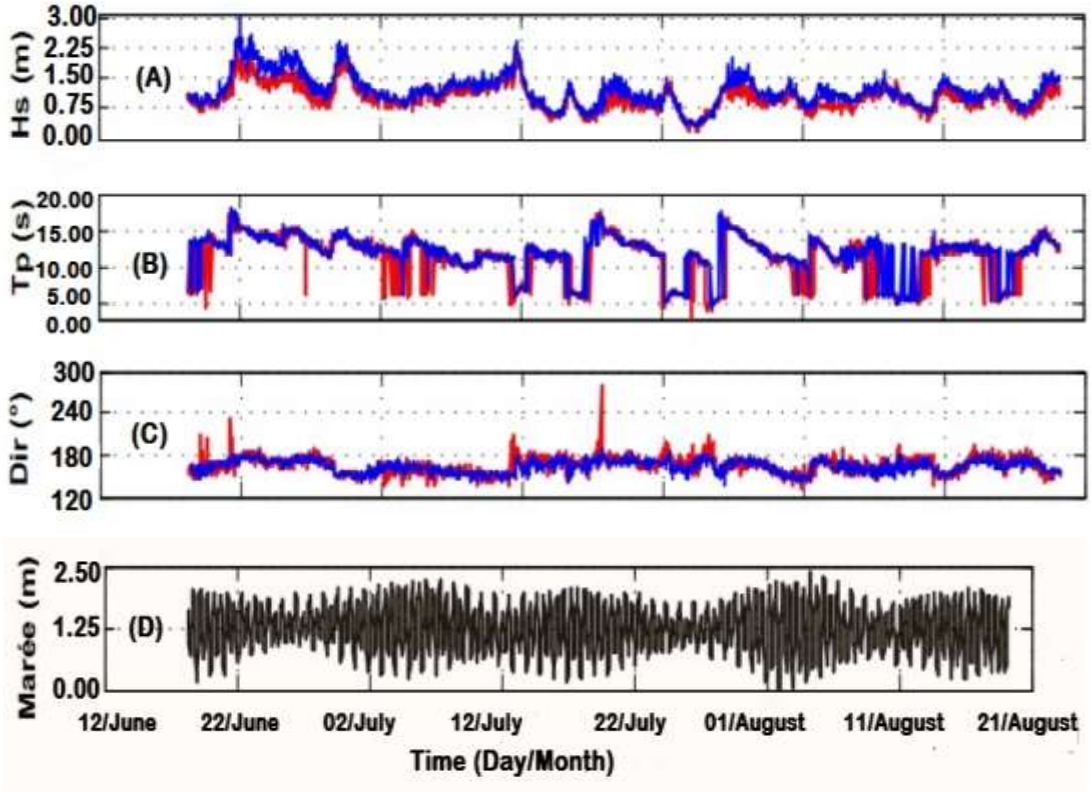

Fig. 3. Temporal evolution of hydrodynamic parameters measured during the measurement campaign at the port of Cotonou. From top to bottom the significant height Hs (m), the peak period Tp (s), the peak direction Dir (°) with station WCP1 in red and station WCP2 in blue, and the variation in sea level (tide) in (m)

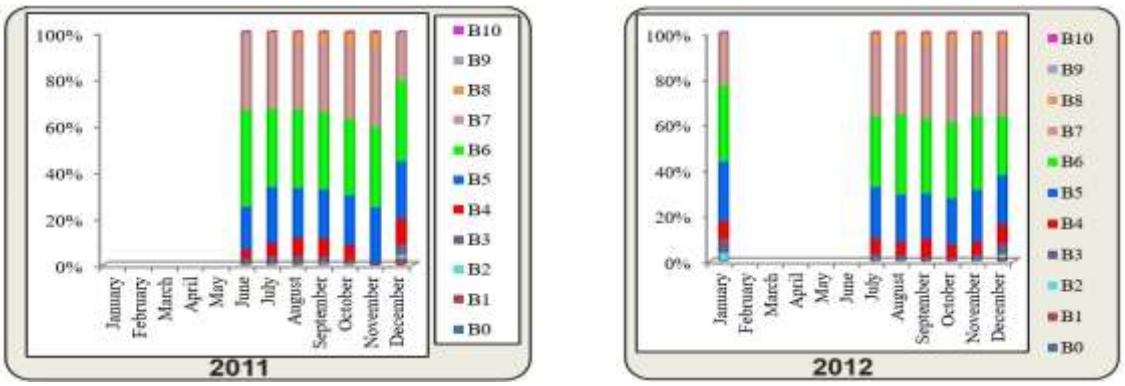

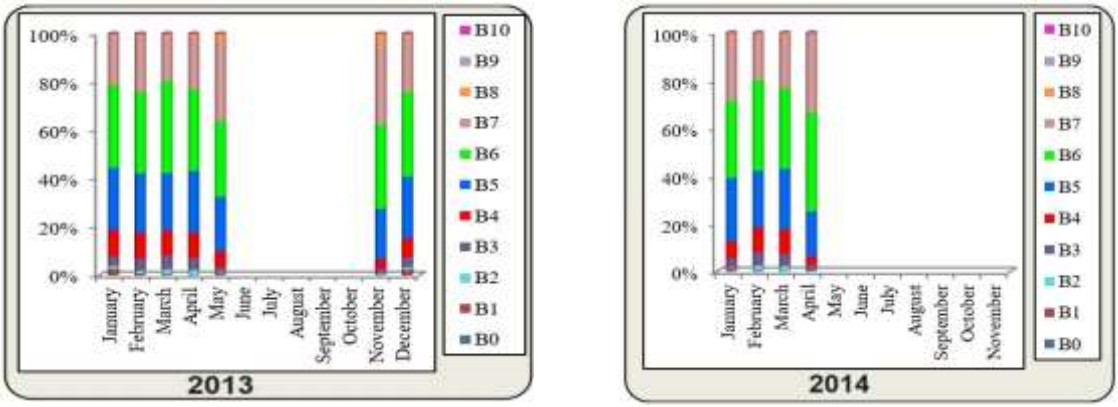

Fig. 4. Monthly distribution of sea states in the coastal zone of Benin in Cotonou from 2011 to 2014

The curves in Fig. 5 below show the maximum H_{max}, minimum H_{min} and significant H_s values of the wave heights during the measurement campaign. The discontinuities observed correspond to months where the measuring devices failed.

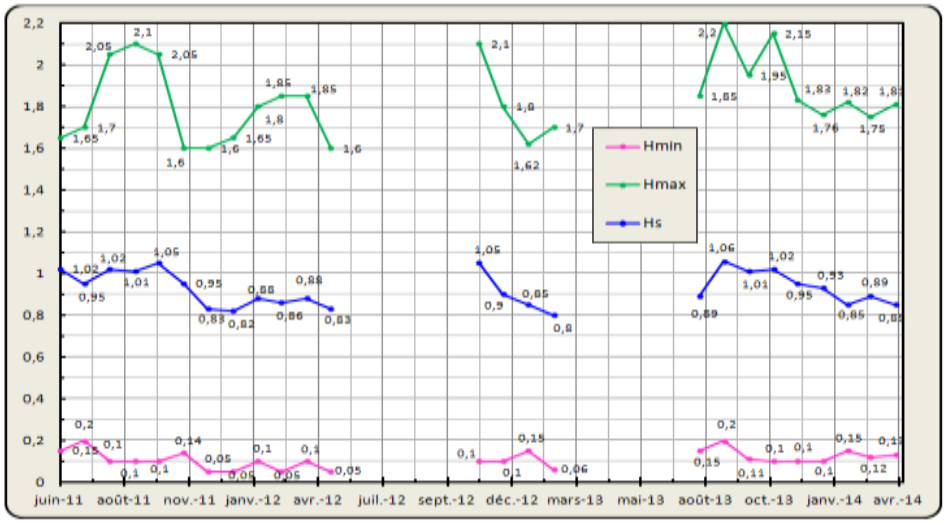

Fig. 5. Variations in maximum, minimum and significant heights from June 2011 to April 2014

The curves in Fig. 6 below show the variations in swell heights, in the deep waters of the coastal zone of the Gulf of Guinea in Benin, as a function of time (GMT hours) during each typical day.

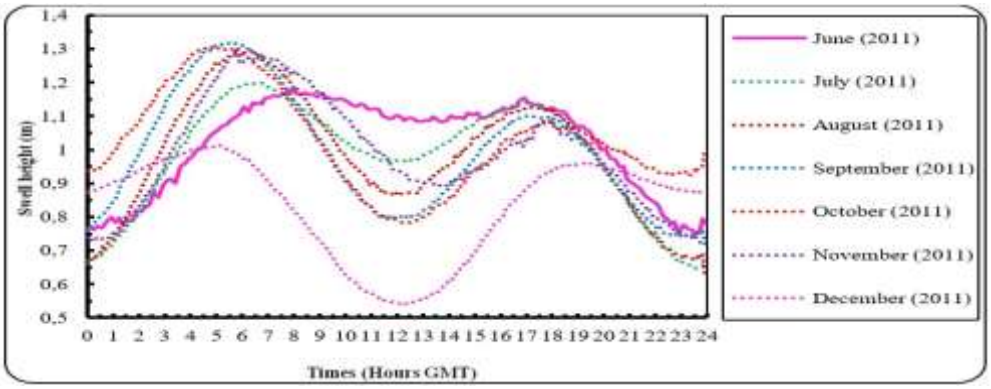

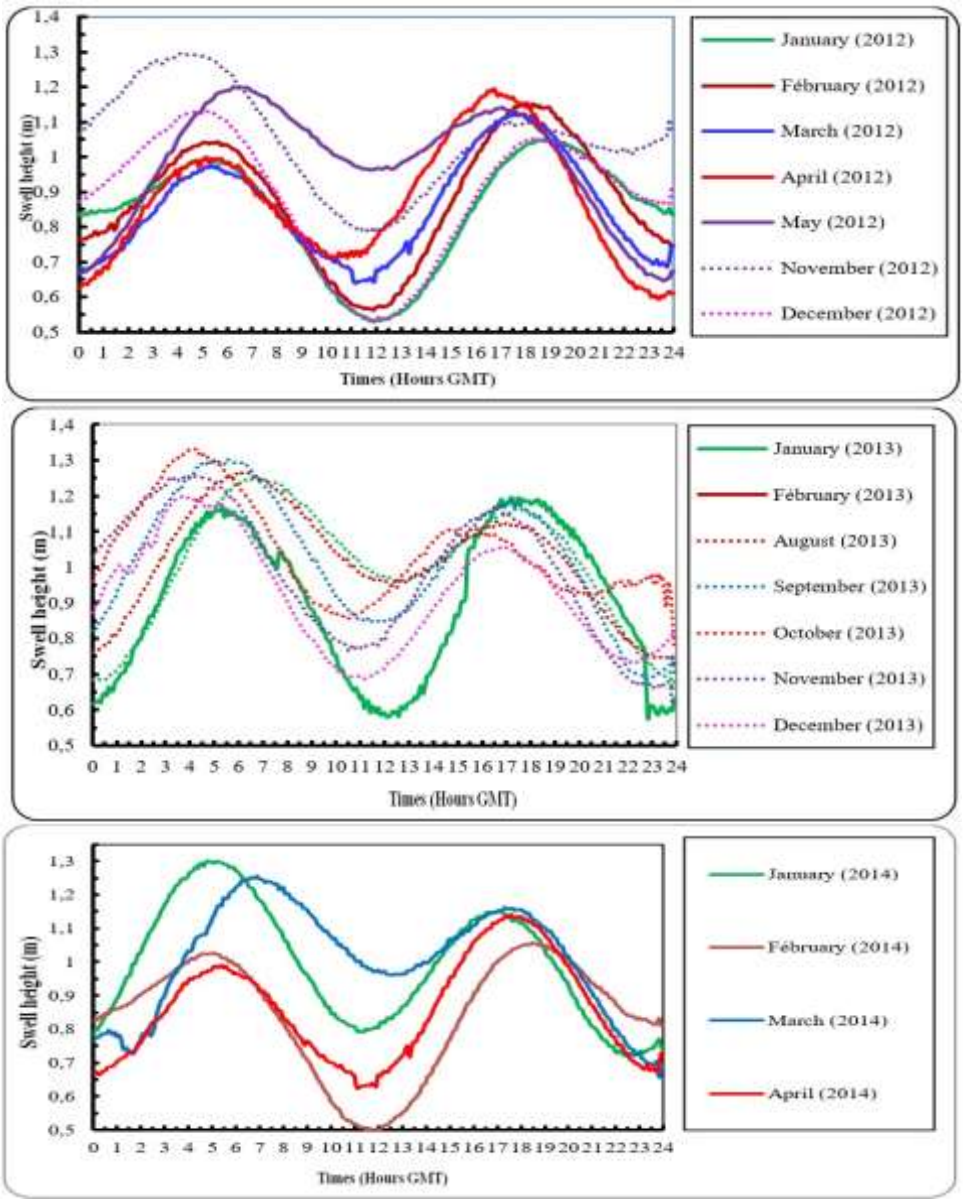

Fig. 6. Swells heights during the typical day from June 2011 to April 2014

The curves in Fig. 7 indicate the variations of the average stable energy power before and after the dissipation of waves or swells as a function of the significant height and the peak period in the study area.

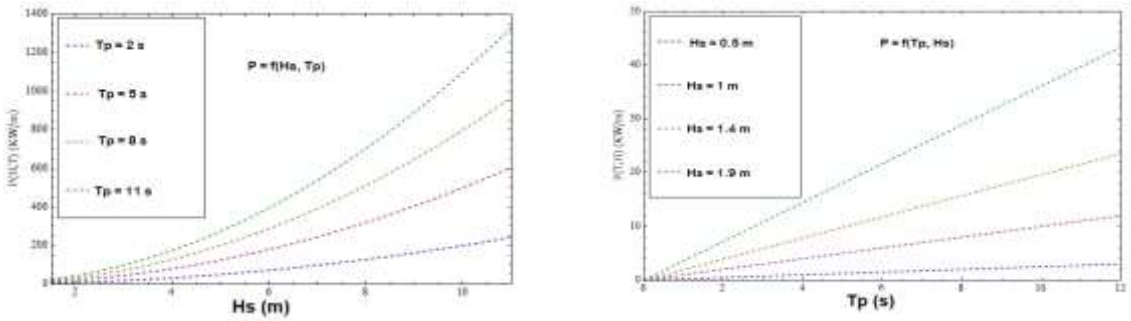

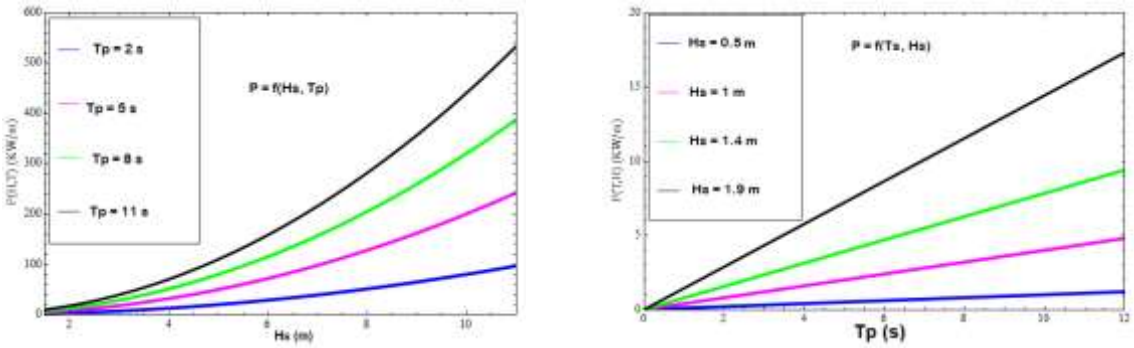

Fig. 7. Variations in stable average energy power before and after waves or swells dissipation in the study area

The curves in **Fig. 8** indicate the energy frequency spectra linked to the pulsation ω and the peak period T_p, where v is wind speed on the fetch at $10m$ from the free surface of the ocean.

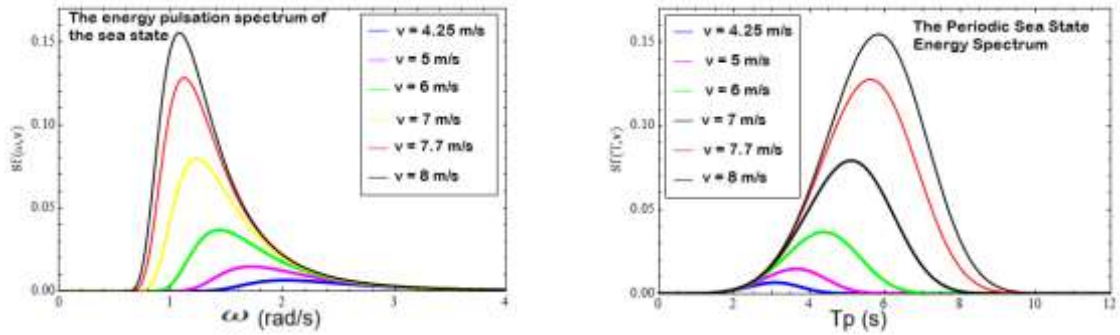

Fig. 8. Energy spectra related to the pulsation ω and the period T_p of the swells of the wind sea in the study area

The curves in **Fig. 9** indicate the wavelength and height of short swells in the study area where v is the wind speed on the fetch at $10m$ from the free surface of the ocean.

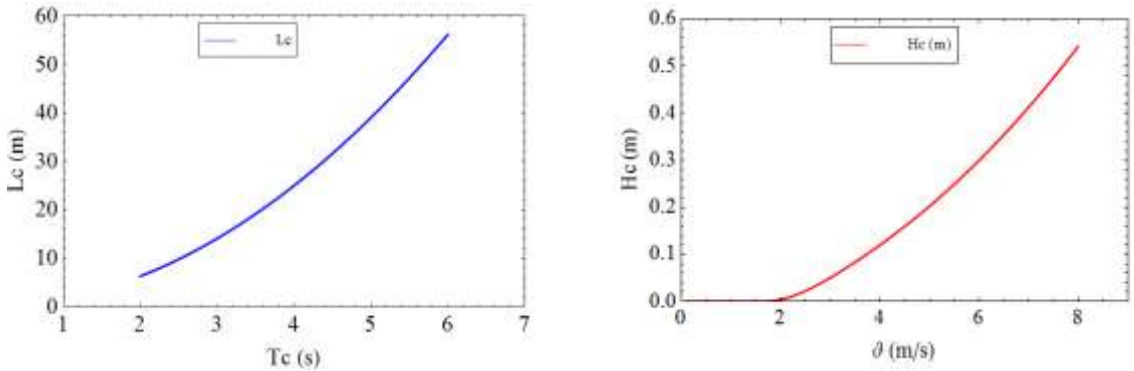

Fig. 9. Variations in wavelength and height of short swells in the study area.

The curves in Fig. 10 indicate variations between the significant height, the peak period and the Beaufort scale in the study area where is wind speed on the fetch at 10m from the free surface of the ocean.

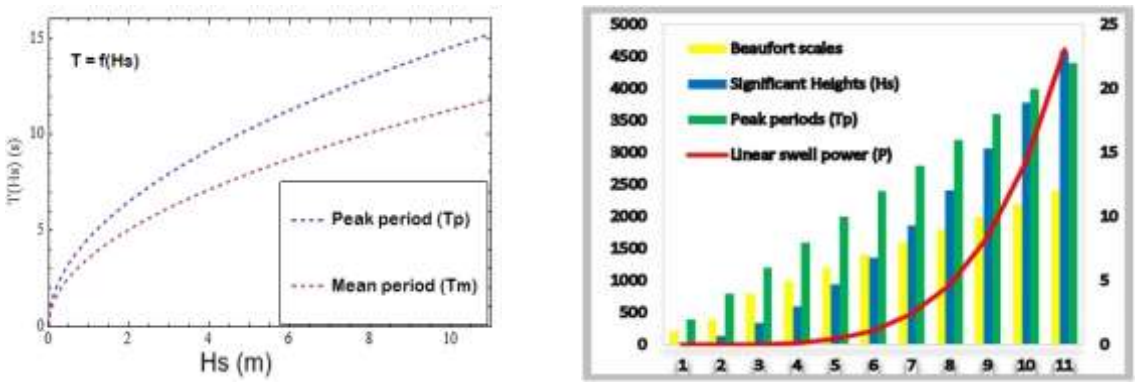

Fig. 10. Variations between significant height, peak period and Beaufort scale in the study area

3.2 Analysis and Discussion of Results

- In Fig. 2, we observe on the one hand the variations in the direction of propagation of the wind during the measurement period (Fig. 2a) and on the other hand a variability of wind speed ranging from 0 to $14m.s^{-1}$ with an average of $5.5m.s^{-1}$. Two maximum wind speeds were obtained on June 21, July 11 and 21 with values of $1.1m.s^{-1}$, $14.2m.s^{-1}$ and $11m.s^{-1}$ respectively (Fig. 2b). These different maxima are associated with the significant height maxima obtained on the same date (Fig. 3A). The winds recorded over this period are on average coming from the SW sector with an average direction of $234°$. Over the recording period only 1.17% of wind speeds are greater than $8.32m.s^{-1}$. The period was characterized by regular breezes from the SW sector.
- We observe a temporal variability of H_s ranging from $0.66m$ to $2.3m$ at the level of the first anchorage (Fig. 3A) and from $0.73m$ to $2.52m$ at the level of the second with respectively averages of 1.22 and $1.32m$ characteristic of wind seas and fairly energetic swells with very energetic sequences on June 22, 28 and July 12 with significant height values of between 1.9 and $2.1m$ at the first anchorage and between 2 and $2.51m$ at the second anchorage. The periods of peak waves observed vary between 3.35 and $17.85s$ with an average of $11.7s$ (Fig. 3B). The significant height maxima observed on June 22, 23 and July 12 are associated with periods of 17.4 respectively ; 16 and $7s$. The direction of the wave peak varies very little (variance : $104°05$ and $58°68$) from an average direction of $197°$ and $196°$ relative to the perpendicular to the coast respectively at the first and second anchorage (swell SWS sector) (Fig. 3C). The analysis of the wave parameter curves makes it possible to identify two phases : the first going from June 17 to July 12 characterized by fairly strong energy waves ($\mathrm{H_{smoy}} > 1.32m$ and $\mathrm{T_{pmoy}} > 11s$). The second phase goes from July 12 to August 18, it is characterized by slightly less energetic waves ($\mathrm{H_{smoy}} < 1.1m$ and $3.4s < T_p < 16s$). The wave periods during the first phase are as high as the significant heights. On the other hand, in the second phase, the wave heights decreased with the increase in wind speed. The tide is the variation in the height of sea level, we observe a high tide and a low tide (Fig. 3D).
- The diagrams in Fig. 4 represent sea states in the Gulf of Guinea at Cotonou. They show that in the coastal zone of Benin :
  - Sea states B_0, B_1, B_9 and B_{10} are almost non-existent (approximately 1%).
  - The B_3, B_4 and B_8 states appear in very low proportions (about 14%).
  - The B_5, B_6 and B_7 states are the most frequent with a strong dominance of the B_6 state (approximately 85%).

All in all, the ocean in the deep waters of the coastal zone of the Gulf of Guinea in Benin is rarely calm ($H = 0$), wrinkled ($0 < H \leq 0.1\ m$) or enormous ($H > 2.29\ m$). It presents at least wavelets ($0.1\ m \leq H < 0.15\ m$) accompanied by small sheep ($0.15\ m \leq H < 0.3\ m$) and sometimes numerous sheep ($0.3\ m \leq H < 0.46\ m$). We frequently observe waves ($0.46\ m \leq$

$H < 0.76\,m$), extensive foam crests ($0.76\,m \leq H < 1.22\,m$) and breaking waves ($1.22\,m \leq H < 1.68\,m$) with strong dominance of extensive foam ridges.

- The curves in Fig. 5 reveal that:
  - The maximum height of the wave heights over the duration of measurements oscillates between $1.6m$ and $2.2m$.
  - Their significant height varies between $0.8m$ and $1.06m$ with an average value of around $0.9m$.
  - As for their minimum value, it is almost zero and oscillates between $0.04m$ and $0.2m$.
- The curves in Fig. 6 represent the evolution of the significant heights of these waves during each typical day. They reveal that these heights vary sinusoidally over the course of a day. These heights take two different maximum values $\mathrm{H_{1max}} \approx 1.3\,\mathrm{m}$ and $\mathrm{H_{2max}} \approx 1.1\,\mathrm{m}$ respectively around 05h and 18h GMT, while they find their minimum values $\mathrm{H_{1min}} \approx 0.6\,\mathrm{m}$ and $\mathrm{H_{2min}} \approx 0.5\,\mathrm{m}$ respectively near $00\mathrm{h}$ and $12\mathrm{h}$ p.m. Their evolution also shows that the swells are regular in Benin. The variations of these heights during any typical day show that the swells in the Gulf of Guinea are regular in Benin and the stable average value of their height varies between $0.5\mathrm{m}$ and $1.3\mathrm{m}$. Over the course of a year, the periods of large swells extend from June to November.
- The curve in Fig. 7 reflects the variations in the energetic power of waves in the deep waters of the coastal zone of Benin. This renewable marine power, available almost permanently, varies between $5\,\mathrm{kW/m}$ and $40\,\mathrm{kW/m}$ when $(0.5\mathrm{m} \leq \mathrm{H_s} \leq 1.4\mathrm{m})$ and $(8s \leq \mathrm{T_p} \leq 18s)$. These waves which have not yet undergone the action of the seabed, will see their energy power increase under the effect of their lifting (shoaling) before their bathymetric surge.
- The curves in Fig. 8 reveal the variations in the energy frequency spectra linked to the pulsation ω and the period $\mathrm{T_p}$ of the wind sea swells in the study area. The spectrum is therefore broken down into its different significant peaks, each corresponding to a wave system. The maximum height of a wave spectrum is higher as there is a larger peak period $\mathrm{T_p}$ and a smaller pulsation ω_p (frequency). Therefore, the energy spectrum $\mathrm{S_\omega}(\omega, \vartheta)$ or $\mathrm{S_f}(\mathrm{T}, \vartheta)$ is an increasing function of the peak period $\mathrm{T_p}$, of the wind speed v and a decreasing function of the pulsation ω_p (frequency).
- The variations of the curves of **Fig. 9**, reveal that the short swells which are generated by the local winds in the coastal zone of Benin, have :
  - A period T_c which varies between $2s$ and $6s$.
  - A wavelength $\mathrm{L_c}$ which oscillates between approximately $10m$ and $55m$.
  - A height $\mathrm{H_c}$ such that $0.1\mathrm{m} \leq \mathrm{H_c} \leq 0.5\mathrm{m}$.
- The curves in **Fig. 10** reveal the variations between the significant height $\mathrm{H_s}$, the peak period $\mathrm{T_p}$ and the Beaufort scale in the study area. The main sea state parameters :
  - The significant height $\mathrm{H_s}$, gives us information on the energy of the waves. Its offshore distribution reveals that off Benin, 94% of the waves have an $\mathrm{H_s}$ of less than $2m$. This analysis of the significant height $\mathrm{H_s}$ allows us to conclude that the sea is not very rough in the Gulf of Guinea.
  - The distribution of the peak period $\mathrm{T_p}$ tells us about the predominant wave system. Off the study area, less than 3% of the waves have a peak period $\mathrm{T_p}$ of less than $9s$ and more than 80% of the waves have a peak period $\mathrm{T_p}$ of between 11 and $15s$. This analysis allows us to conclude that swells are the wave systems that predominate in the northern Gulf of Guinea in more than 90% of cases.

In general, our results found are in agreement with those obtained in the literature especially by [24], [25], [31]. The difference observed lies in the fact that in the Gulf of Guinea, there are no strong winds to generate wind seas (wind speeds are on average around $5\,m/s$) [32] and that the basin is open towards the south and west allowing swells coming from these sectors to propagate without encountering any obstacle.

4. CONCLUSION

Using high quality data from two measuring stations (station WCP1 and station WCP2), we can conclude that:

A statistical analysis made on the different wave parameters shows that 81% and 90% of the

significant heights recorded were greater than $1.1m$ respectively at the WCP1 and WCP2 stations during the measurement period. The distribution of Hs at station WCP1 is quite different from that obtained by station WCP2. In particular, we observe a higher percentage of larger events involving significant heights greater than $1.8m$ for station WCP2. Also, 77% and 82% of wave peak periods were greater than $8.1s$ at stations WCP1 and WCP2 respectively. During the measurement campaign, this area was exposed to long swells, i.e. waves generated further from the observation point, therefore from the South Atlantic, associated with high periods ($T_p > 8.1s$). The presence of locally generated wind seas in the Gulf of Guinea associated with periods less than $8.1s$ have been detected, particularly during the second phase identified above. The main characteristic of the peak direction obtained during the measurement campaign is its very narrow distribution. Indeed, more than 85% of this direction is included in an angular sector of $30°$. We note on average a direction which is that of the SWS sector ($196°5$ compared to the normal to the coast) therefore an average incidence of waves of $16°5$. This study also reveals that the coastal zone of the Gulf of Guinea is characterized by an abundance of moderate waves taking a more clearly elongated shape, crests of white foam and breaking waves whose average stable heights (significant heights) vary between $0.5m$ and $1.4m$. Their main direction of propagation is south-southwest (SSW). These waves have a period which varies between $8s$ and $18s$ with a stable average value of $12s$. In this area, wavelets, sheep ($\mathrm{H} < 0.46\,m$) and swell crests starting in whirlwinds of foam ($\mathrm{H} > 1.7\,m$) are rarely present. The energetic power of these waves oscillates between $5\ \mathrm{kW/m}$ and $40\ \mathrm{kW/m}$. As for short swells (wind seas) generated by local winds, they have a period ($2s \leq T_c \leq 6s$), a wavelength of $10m \leq L_c \leq 55m$ and their height varies between $0.1m$ and $0.5m$. Short swells (wind seas) generated by local winds. Their wavelength $L_c \leq 55m$ and their period $T_c \leq 6s$. These swells are frequent and often generate micro-turbulences on the ocean surface.

In general, the state of the seas in the North of the Gulf of Guinea is quite homogeneous with a system made up of swell (more than 85%) coming from the South Atlantic. The most likely periods are between $12s$ and $14s$. The numbers show a predominance of the south-southwest sector for the swells off Benin, likewise in terms of Hs. Apart from a few exceptional events, these swells have a moderate Hs of around 1.5 to $2m$. The most probable sea state consists of a wave of significant height Hs close to $1.8m$ and a period close to $13.5s$. As the peak period T_p increases, the frequency spectrum increases. So, the frequency spectrum is an increasing function of the peak period T_p. It can be seen that the level of energy carried by the waves is highly variable depending on the state of the sea, and can reach considerable power levels in the event of strong storms.

DATA AVAILABILITY

The datasets generated during and/or analyzed during the current study are available from the authors on reasonable request.

ACKNOWLEDGEMENTS

The authors are indebted to the Institute of Halieutic and Oceanological Research of Benin (IRHOB) / Beninese Center for Scientific Research and Innovation (CBRSI) for the buoy data and the support of this research work.

COMPETING INTERESTS

Authors have declared that no competing interests exist.

REFERENCES

1. Larson ER, Mirti T, Wilding T, Underwood CA. Five Centuries of Groundwater Elevations Provide Evidence of Shifting Climate Drivers and Human Influences on Water Resources in North Central Florida. Water Resources Research. 2023 Sep;59(9):e2022WR031970.
DOI: 10.1029/2022WR031970.
2. Amores A, Marcos M, Carrió DS, Gómez-Pujol L. Coastal impacts of Storm Gloria (January 2020) over the north-western Mediterranean. Natural Hazards and Earth System Sciences. 2020;20(7):1955-68.
DOI: 10.5194/nhess-20-1955-2020.
3. Amores A, Melnichenko O, Maximenko N. Coherent mesoscale eddies in the N orth A tlantic subtropical gyre: 3-D structure and transport with application to the salinity maximum. Journal of Geophysical Research: Oceans. 2017;122(1):23-41.
DOI: 10.1002/2016JC012256.

4. Tokpohozin NB, Fannou JLC, Houekpoheha AM, Houngue HG, Kounouhewa BB, Statistical Study of wave parameters : Sea states in the deep waters (Offshore) of the gulf of Guinea In Benin. Int. J. Curr. Res. 2023 ;15(nº 02):23709-23719.
DOI: 10.24941/ijcr.44701.02.2023.
5. Acclassato OG, Tokpohozin NB, Akowanou CD, Houékpohéha AM, Houngue GH, Kounouhéwa BB. Study of Dissipating of Wave Energy in the Breakers Zone of the Gulf of Guinea: Case of Autonomous Port of Cotonou in Benin Coastal Zone. Journal of Modern Physics. 2022;13(9):1272-86.
DOI: 10.4236/jmp.2022.139076.
6. Tokpohozin NB, Kounouhewa B, Avossevou GY, Houekpoheham A, Awanou CN. Modelling of sediment movement in the surf and swash zones. Acta Oceanologica Sinica. 2015;34(2):137-42.
DOI: 10.1007/s13131-015-0610-2.
7. Yu L. Global variations in oceanic evaporation (1958–2005): The role of the changing wind speed. Journal of climate. 2007;20(21):5376-90.
DOI: 10.1175/2007JCLI1714.1.
8. Ardhuin F, Chapron B, Collard F. Observation of swell dissipation across oceans. Geophysical Research Letters. 2009;36(6).
DOI: 10.1029/2008GL037030.
9. Xu Y, Yu X. Enhanced formulation of wind energy input into waves in developing sea. Progress in Oceanography. 2020;186:102376.
DOI: 10.1016/j.pocean.2020.102376.
10. Semedo A, Sušelj K, Rutgersson A, Sterl A. A global view on the wind sea and swell climate and variability from ERA-40. Journal of Climate. 2011;24(5):1461-79.
DOI: 10.1175/2010JCLI3718.1.
11. Alves JH. Numerical modeling of ocean swell contributions to the global wind-wave climate. Ocean Modelling. 2006;11(1-2):98-122.
DOI: 10.1016/j.ocemod.2004.11.007.
12. Liu Q, Rogers WE, Babanin AV, Young IR, Romero L, Zieger S, Qiao F, Guan C. Observation-based source terms in the third-generation wave model WAVEWATCH III: Updates and verification. Journal of Physical Oceanography. 2019;49(2):489-517.
DOI: 10.1175/JPO-D-18-0137.1.
13. Alves JH. Numerical modeling of ocean swell contributions to the global wind-wave climate. Ocean Modelling. 2006;11(1-2):98-122.
14. Castelao RM. Mesoscale eddies in the South Atlantic Bight and the Gulf Stream recirculation region: vertical structure. Journal of Geophysical Research: Oceans. 2014;119(3):2048-65.,
DOI: 10.1002/2014JC009796.
15. Houekpoheha MA, Kounouhewa BB, Hounsou JT, Tokpohozin BN, Hounguevou JV, Awanou CN. Variations of wave energy power in shoaling zone of Benin coastal zone. International Journal of Renewable Energy Development. 2015;4(1):64.
DOI: 10.14710/ijred.4.1.64-71.
16. Hervé Hounguè G, Kounouhewa BB, Almar R, Sohou Z, Lefebvre JP, Houépkonhéha M, Tokpohozin B. Waves forcing climate on Benin coast, and the link with climatic index, Gulf of Guinea (West Africa). Journal of Coastal Research. 2018 ;81:130-7.
DOI: 10.2112/SI81-017.1.
17. Bishop CT, Donelan MA. Chapter 4 Wave Prediction Models. In Elsevier Oceanography Series. 1989;49(Elsevier): 75-105.
DOI: 10.1016/S0422-9894(08)70124-7.
18. Vanem E, Zhu T, Babanin A. Statistical modelling of the ocean environment–A review of recent developments in theory and applications. Marine Structures. 2022;86:103297.
DOI: 10.1016/j.marstruc.2022.103297.
19. Bromirski PD, Cayan DR, Flick RE. Wave spectral energy variability in the northeast Pacific. Journal of Geophysical Research: Oceans. 2005;110(C3).
DOI: 10.1029/2004JC002398.
20. Hwang PA, Ocampo-Torres FJ, García-Nava H. Wind sea and swell separation of 1D wave spectrum by a spectrum integration method. Journal of Atmospheric and Oceanic Technology. 2012 Jan 1;29(1):116-28.
DOI: 10.1175/JTECH-D-11-00075.1.
21. Tréguier AM, Deshayes J, Lique C, Dussin R, Molines JM. Eddy contributions to the meridional transport of salt in the North Atlantic. Journal of Geophysical Research: Oceans. 2012;117(C5).
DOI: 10.1029/2012JC007927.
22. Niayifar A, Porté-Agel F. Analytical modeling of wind farms: A new approach

for power prediction. Energies. 2016; 9(9):741.
DOI: 10.3390/en9090741.

23. Caires S, Sterl A. Validation of ocean wind and wave data using triple collocation. Journal of geophysical research: oceans. 2003;108(C3).
DOI: 10.1029/2002JC001491.

24. Kim J, Kim JA, McGinty RK, Nguyen UT, Muir TW, Allis CD, Roeder RG. The n-SET domain of Set1 regulates H2B ubiquitylation-dependent H3K4 methylation. Molecular cell. 2013 Mar 28;49(6):1121-33.
DOI: 10.1016/j.molcel.2013.01.034.

25. Almar R, Hounkonnou N, Anthony EJ, Castelle B, Senechal N, Laibi R, Mensah-Senoo T, Degbe G, Quenum M, Dorel M, Chuchla R. The Grand Popo beach 2013 experiment, Benin, West Africa: from short timescale processes to their integrated impact over long-term coastal evolution. Journal of Coastal Research. 2014 (70):651-6.
DOI: 10.2112/SI70-110.1.

26. Li XM, Huang B. A global sea state dataset from spaceborne synthetic aperture radar wave mode data. Scientific data. 2020;7(1):261.
DOI: 10.1038/s41597-020-00601-3.

27. Marc P. Animation phénoménologique de la mer — une approche énactive. Bretagne Occidentale, Ecole Doctorale SMIS, sp´ecialit´e : Informatique ; 2004.

28. Shemer L, Sergeeva A. An experimental study of spatial evolution of statistical parameters in a unidirectional narrow-banded random wavefield. Journal of Geophysical Research: Oceans. 2009;114(C1).
DOI: 10.1029/2008JC005077.

29. Babarit A, Hals J, Muliawan MJ, Kurniawan A, Moan T, Krokstad J. Numerical benchmarking study of a selection of wave energy converters. Renewable energy. 2012;41:44-63.
DOI: 10.1016/j.renene.2011.10.002.

30. Liu G, Chen Z, Lu H, Liu Z, Zhang Q, He Q, He Y, Xu J, Gong Y, Cai S. Energy Transfer Between Mesoscale Eddies and Near-Inertial Waves From Surface Drifter Observations. Geophysical Research Letters. 2023;50(16):e2023GL104729.

31. Chen G, Chapron B, Ezraty R, Vandemark D. A global view of swell and wind sea climate in the ocean by satellite altimeter and scatterometer. Journal of Atmospheric and Oceanic Technology. 2002;19(11):1849-59.

32. Laibi R. Dynamique actuelle d'une embouchure fluviale estuarienne à flèche sableuse: la bouche du Roi, Bénin, Golfe de Guinée. Résumé de la thèse de Doctorat, UAC. 2011 ;10.

Peer-review history:
The peer review history for this paper can be accessed here:
https://www.sdiarticle5.com/review-history/108047